Cosmic rays and indirect dark matter detection

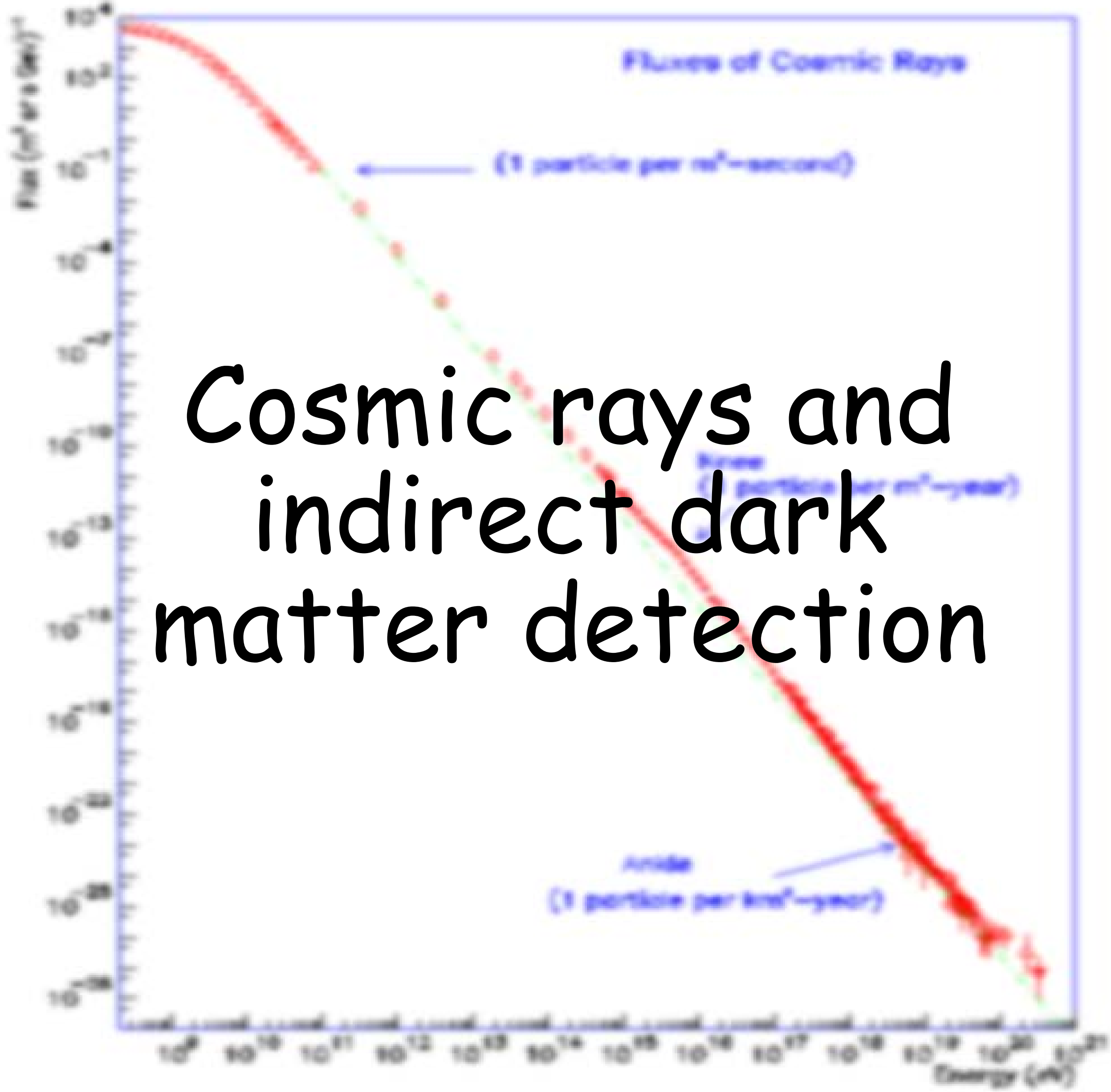

Cosmic Rays

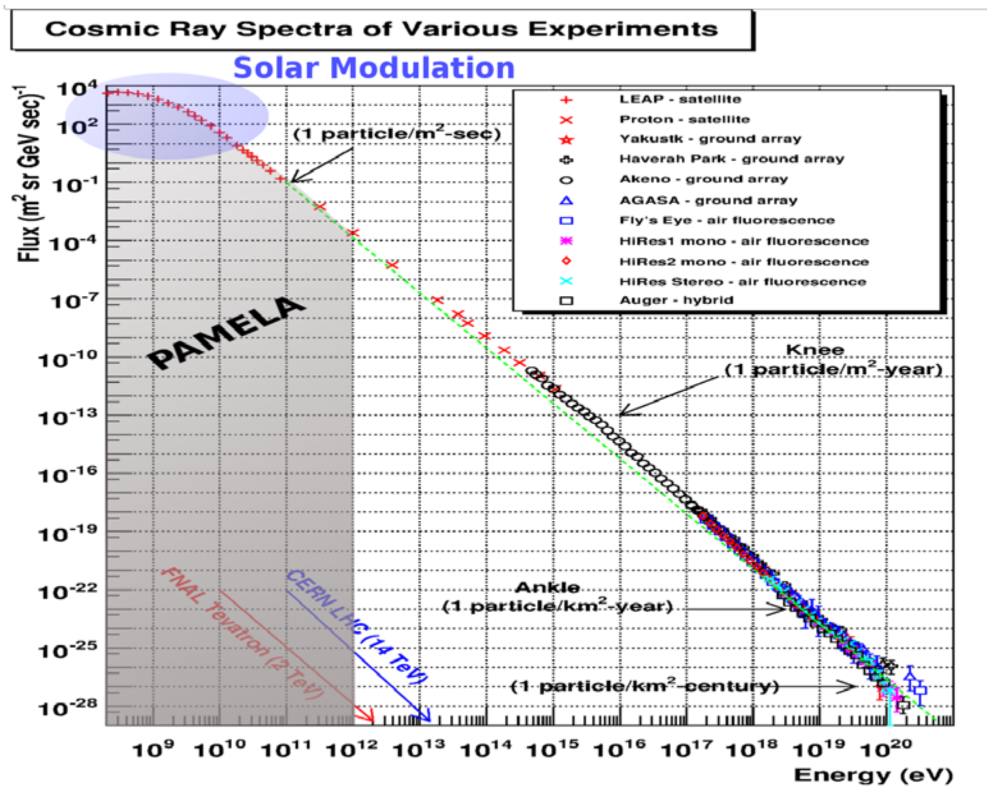
Cosmic Ray Spectra of Various Experiments
Solar Modulation
Flux (m² sr GeV sec)⁻¹
(1 particle/m²-sec)
LEAP - satellite
Proton - satellite
Yakustk - ground array
Haverah Park - ground array
Akeno - ground array
AGASA - ground array
Fly's Eye - air fluorescence
HiRes1 mono - air fluorescence
HiRes2 mono - air fluorescence
HiRes Stereo - air fluorescence
Auger - hybrid
PAMELA
Knee
(1 particle/m²-year)
Ankle
(1 particle/km²-year)
FNAL Tevatron (2 TeV)
CERN LHC (14 TeV)
(1 particle/km²-century)
Energy (eV)

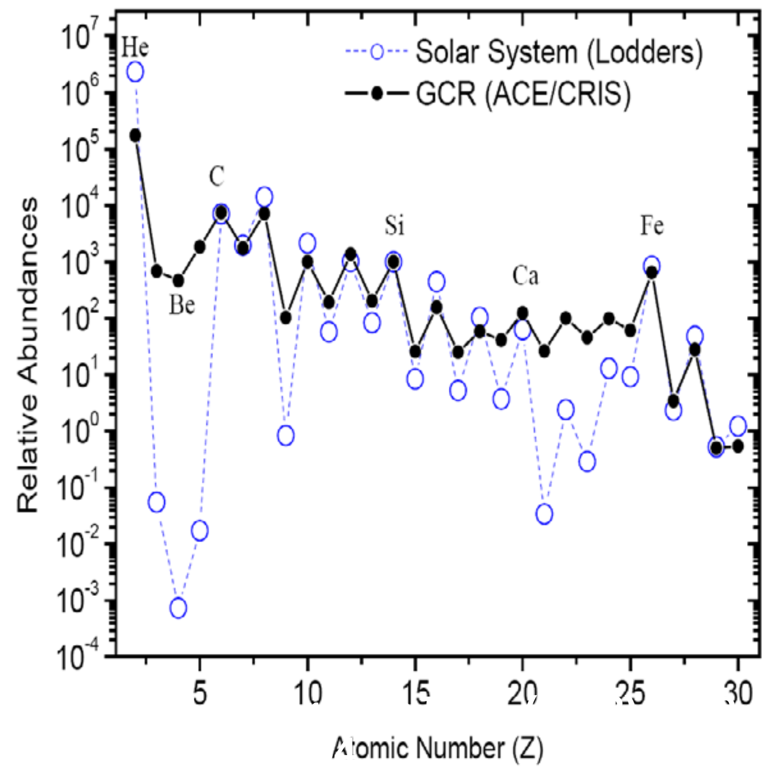
Solar System (Lodders)
GCR (ACE/CRIS)
He
C
Be
Si
Ca
Fe
Relative Abundances
Atomic Number (Z)

Galactic DM signals

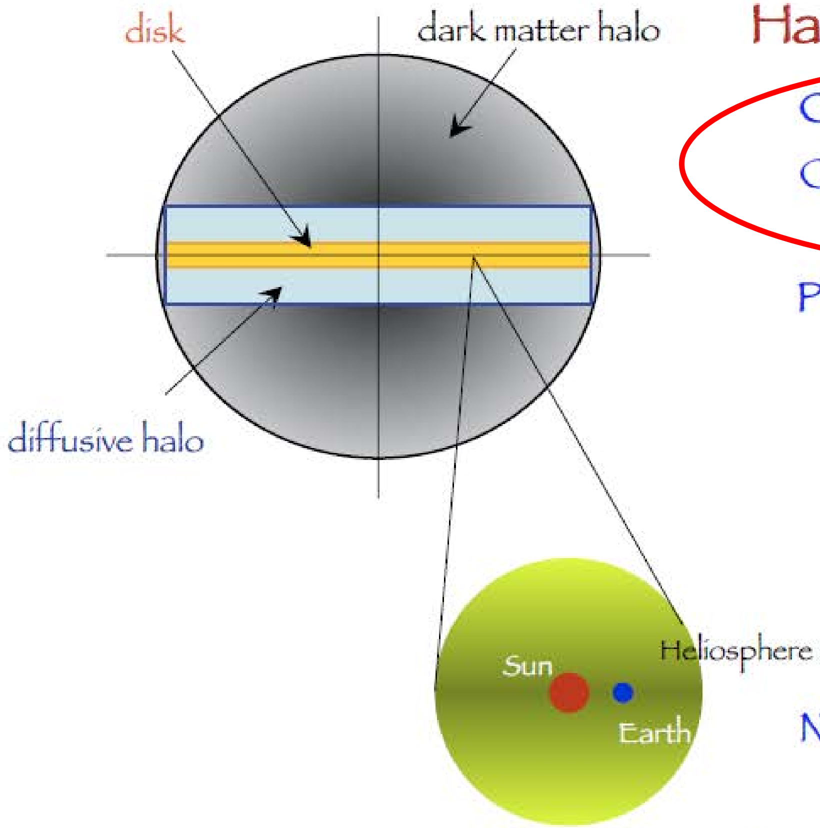

Halo signals

Charged Leptonic CR: $e^{\pm}$

Charged Baryonic CR: antiP, antiD, antiHe

Photons

- Gamma-rays
  - Prompt production
  - IC from $e^{\pm}$ on ISRF and CMB
- X-rays
  - IC from $e^{\pm}$ on ISRF and CMB
- Radio
  - Synchro from $e^{\pm}$ on mag. field

Neutrinos

Local signals

Direct detection

Neutrinos from Earth and Sun

Courtesy by N. Fornengo

Cosmic Rays and Anti-Particles

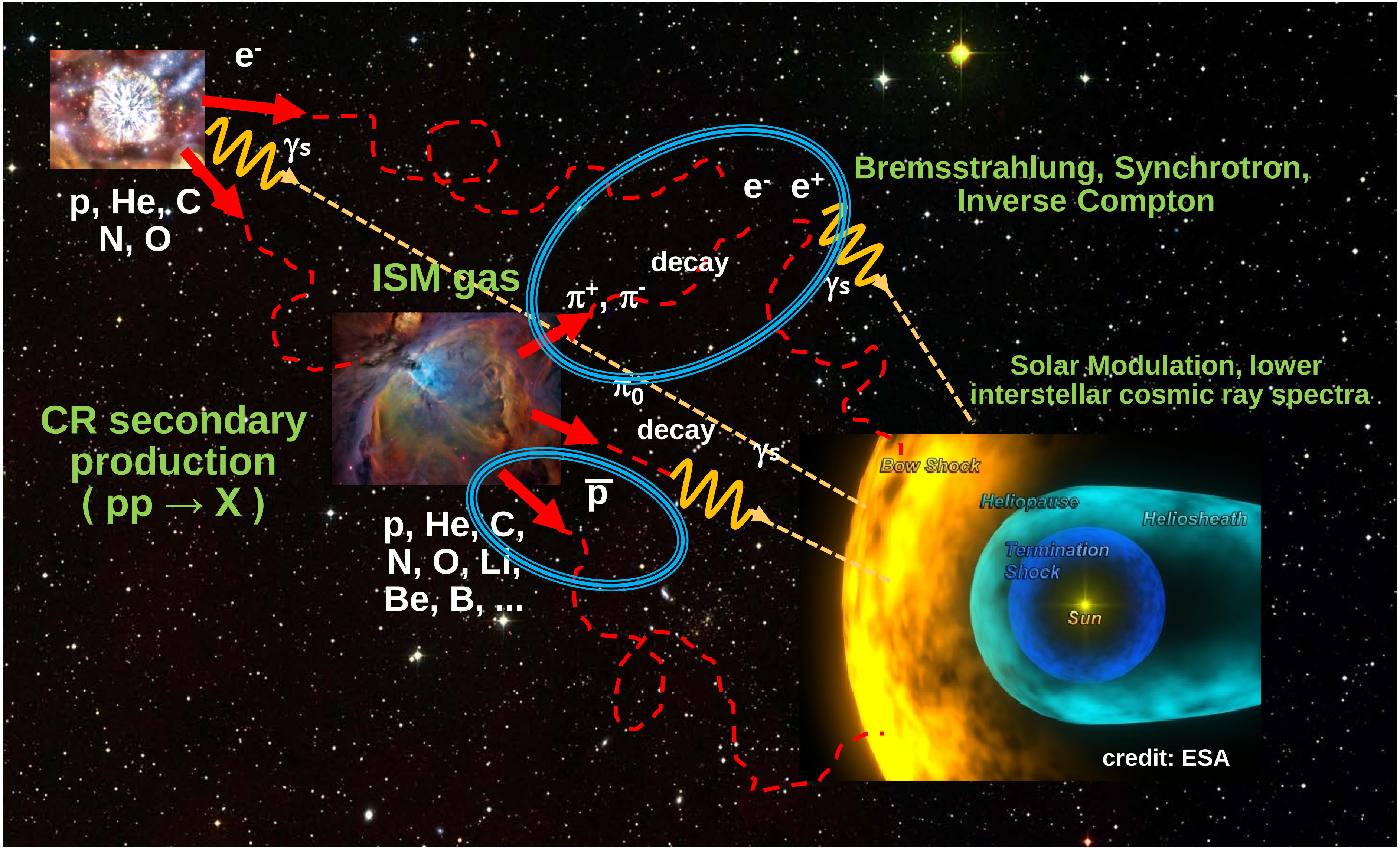

Pillars of the SNR paradigm

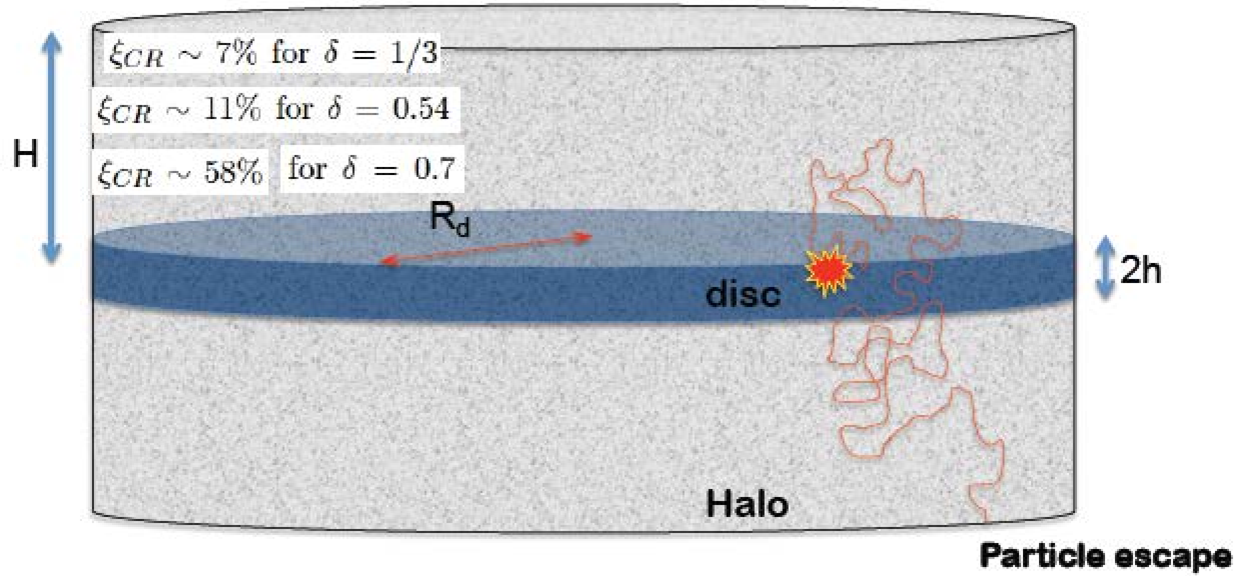

CRs IN SNR → DIFFUSIVE SHOCK ACCELERATION, Q(E)~$E^{-\gamma}$

PROPAGATION OF CRs IN THE GALAXY with D(E)~E^{δ} → n(E)~$E^{-\gamma-\delta}$

P. Blasi, TeVPA 2011, Stockholm 2011

Positron to Electron Fraction

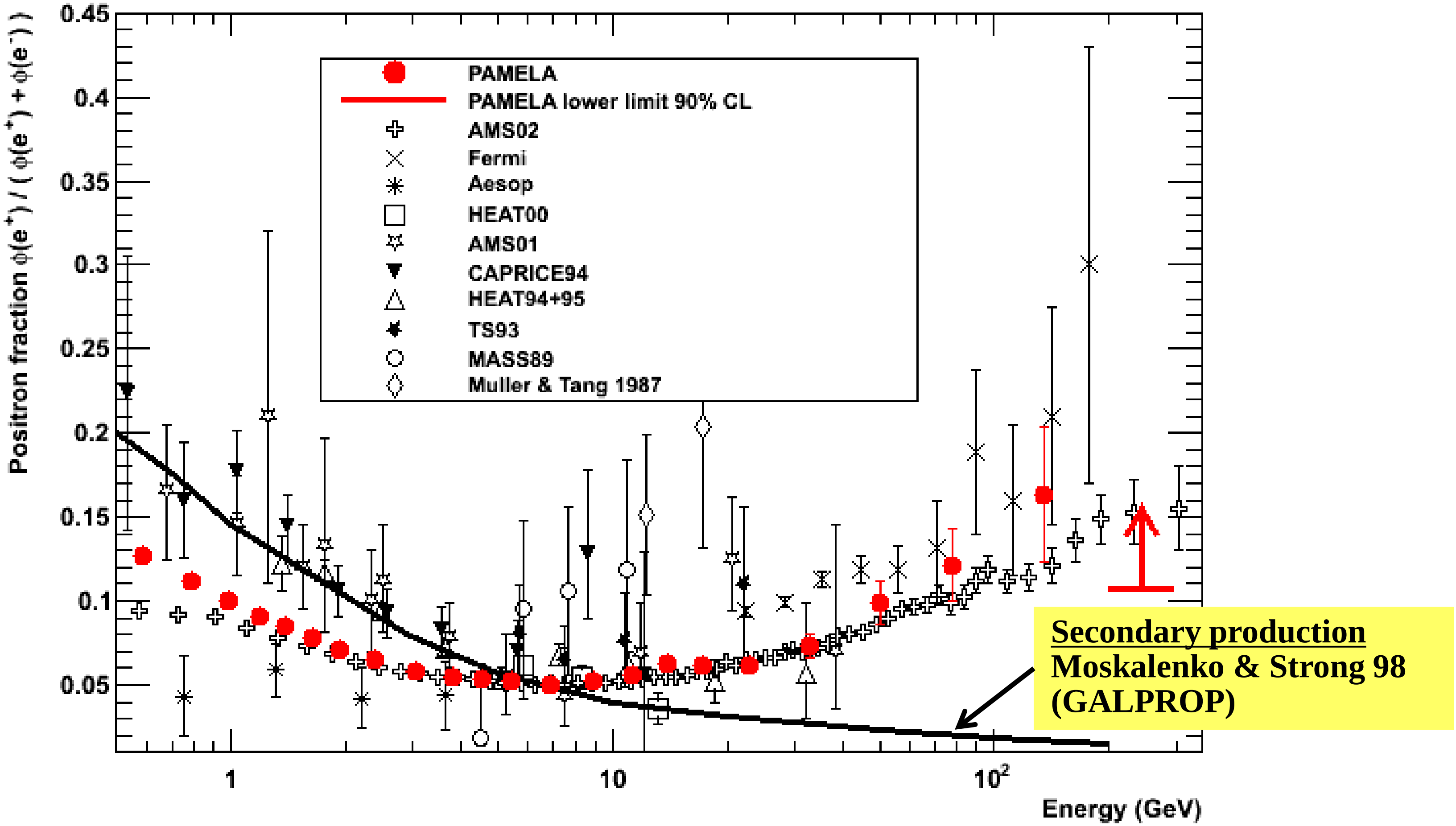

Secondary positrons (1)

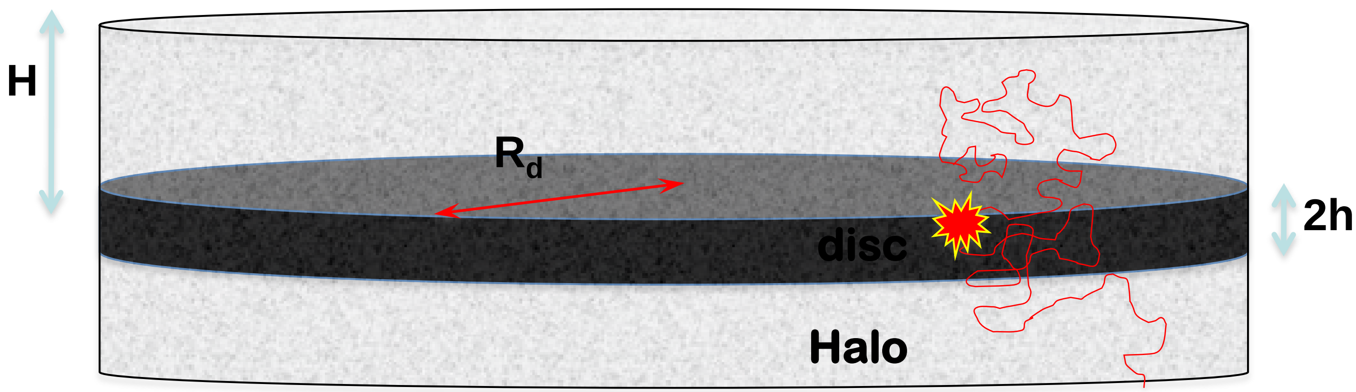

PRIMARY COSMIC RAY SPECTRUM AT EARTH

$$n_{CR}(E) = \frac{N(E)\mathcal{R}}{2\pi R_d^2}\frac{H}{D(E)} \equiv \frac{N(E)\mathcal{R}}{2H\pi R_d^2}\frac{H^2}{D(E)} \propto E^{-\gamma-\delta}$$

SPECTRUM OF PRIMARY ELECTRONS AT EARTH

$$n_e(E) \approx \frac{N(E)\Re\,\tau_{loss}(E)}{\sqrt{D(E)\tau_{loss}(E)}} \propto E^{-\gamma-1/2-\delta/2}$$

IF ENERGY LOSSES ARE DOMINANT UPON DIFFUSION (TYPICALLY E>10 GeV

Courtesy by P. Blasi

Secondary positrons (2)

INJECTION RATE OF SECONDARY POSITRONS

$$q_{e^+}(E')dE' = n_{CR}(E)dE\, n_H\, \sigma_{pp}\, c \propto E^{-\gamma-\delta}$$

EQUILIBRIUM SPECTRUM OF SECONDARY POSITRONS (AND ELECTRONS) AT EARTH

$$n_{e^+}(E) \approx \frac{q_{e^+}(E)\tau_{loss}(E)}{\sqrt{D(E)\tau_{loss}(E)}} \propto E^{-\gamma-1/2-3\delta/2}$$

POSITRON FRACTION

$$\boxed{\frac{\Phi_{e^+}}{\Phi_{e^+}+\Phi_{e^-}} \approx \frac{\Phi_{e^+}}{\Phi_{e^-}} \propto E^{-\delta}}$$

MONOTONICALLY DECREASING FUNCTION OF ENERGY

Courtesy by P. Blasi

Extended gamma-ray sources around pulsars constrain the origin of the positron flux at Earth

A. U. Abeysekara,[1] A. Albert,[2] R. Alfaro,[3] C. Alvarez,[4] J. D. Álvarez,[5] R. Arceo,[4]

We report the detection, using the High-Altitude Water Cherenkov Observatory(HAWC), of extended tera–electron volt gamma-ray emission coincident with the locations of two nearby middle-aged pulsars (Geminga and PSR B0656+14). The HAWC observations demonstrate that these pulsars are indeed local sources of accelerated leptons, but the measured tera–electron volt emission profile constrains the diffusion of particles away from these sources to be much slower than previously assumed. **We demonstrate that the leptons emitted by these objects are therefore unlikely to be the origin of the excess positrons, which may have a more exotic origin.**

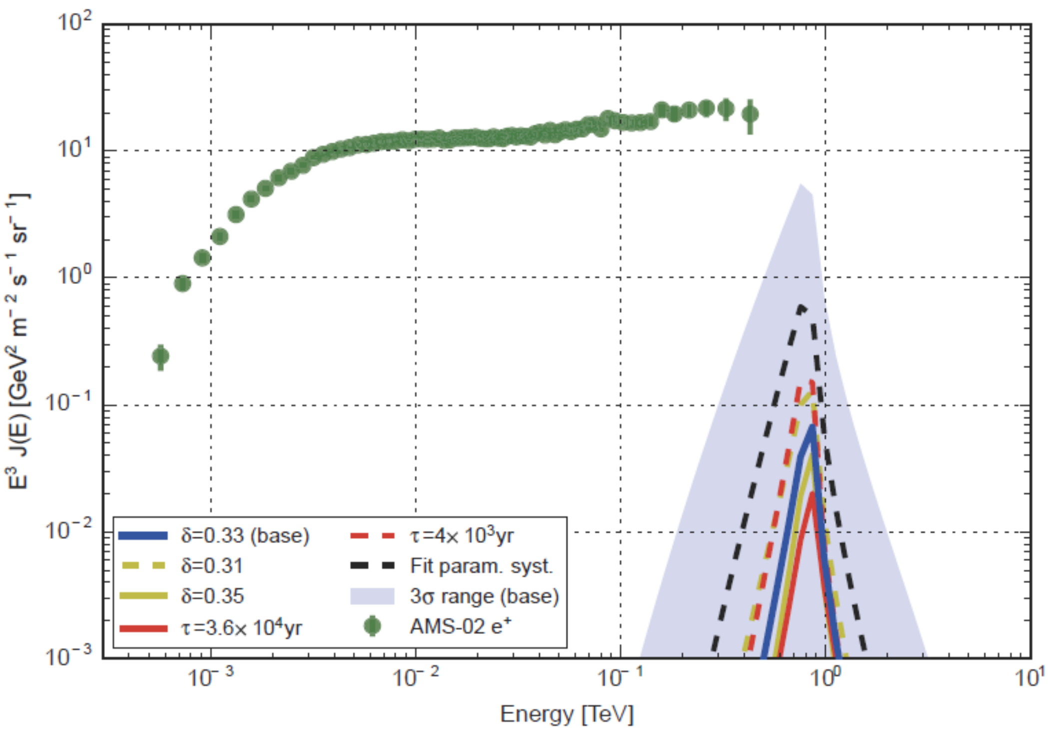

Fig. 3. Estimated positron energy flux at Earth from Geminga (blue solid line), compared with AMS-02 experimental measurements (green dots). The shaded blue region indicates the 3σ (99.5% confidence) statistical uncertainty from simulations (*12*). Additional lines represent the effect

But see also: e.g.
D. Hooper & T. Linden, arXiv:1711.07482

Anisotropy in the PAMELA e+ and e- data

Positrons - R > 10 GV

Significance map for *backtraced* positrons
Background: Protons
Angular scale 10°

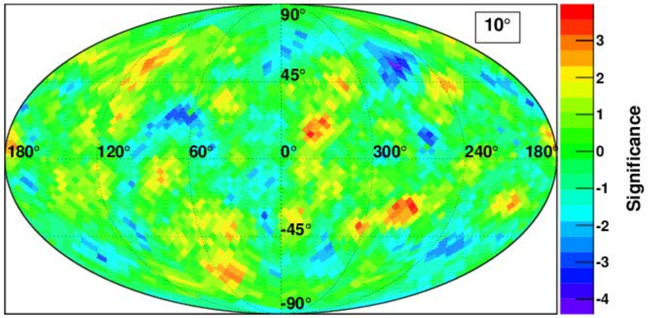

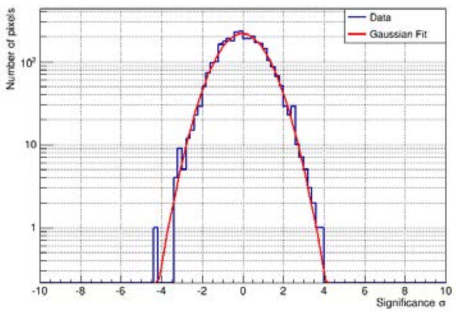

Histogram of calculated significance

Electrons R > 10 GV

Significance map for *backtraced* electrons
Background: Monte Carlo simulations
Angular scale 10°

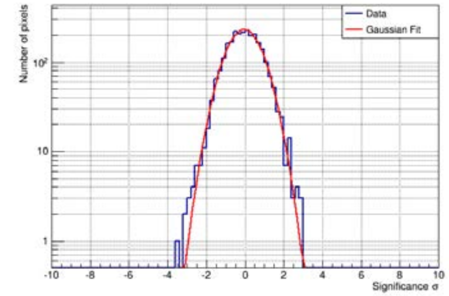

Histogram of calculated significance

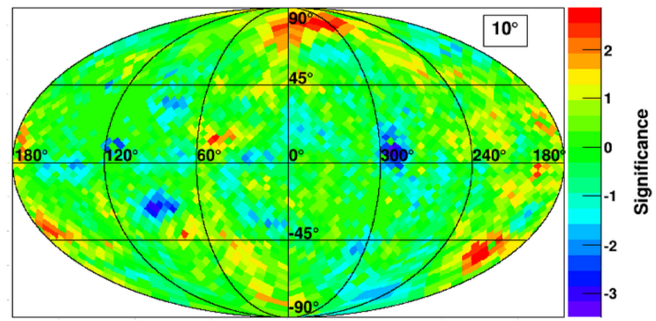

O. Adriani et al., ApJ 811 (2015) 21

Number of events as a function of the angular distance from the Sun direction

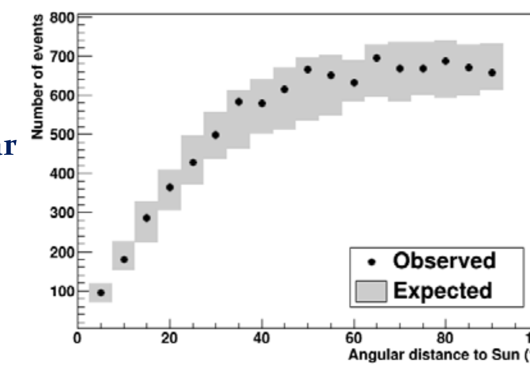

Antiproton results: PAMELA vs BESS Polar & AMS-02

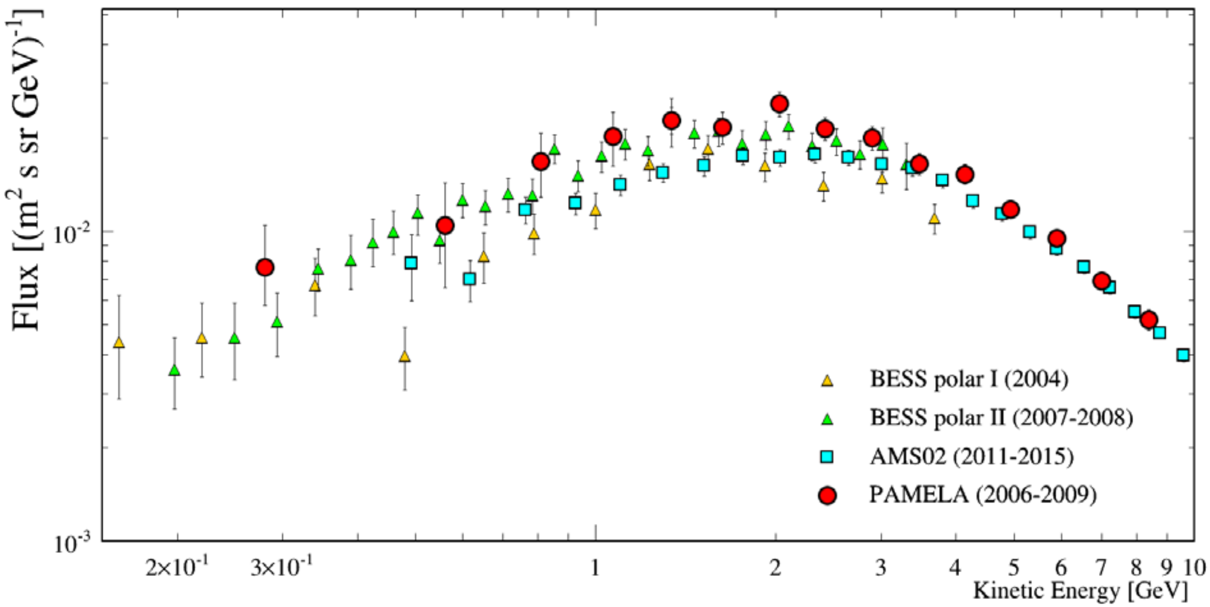

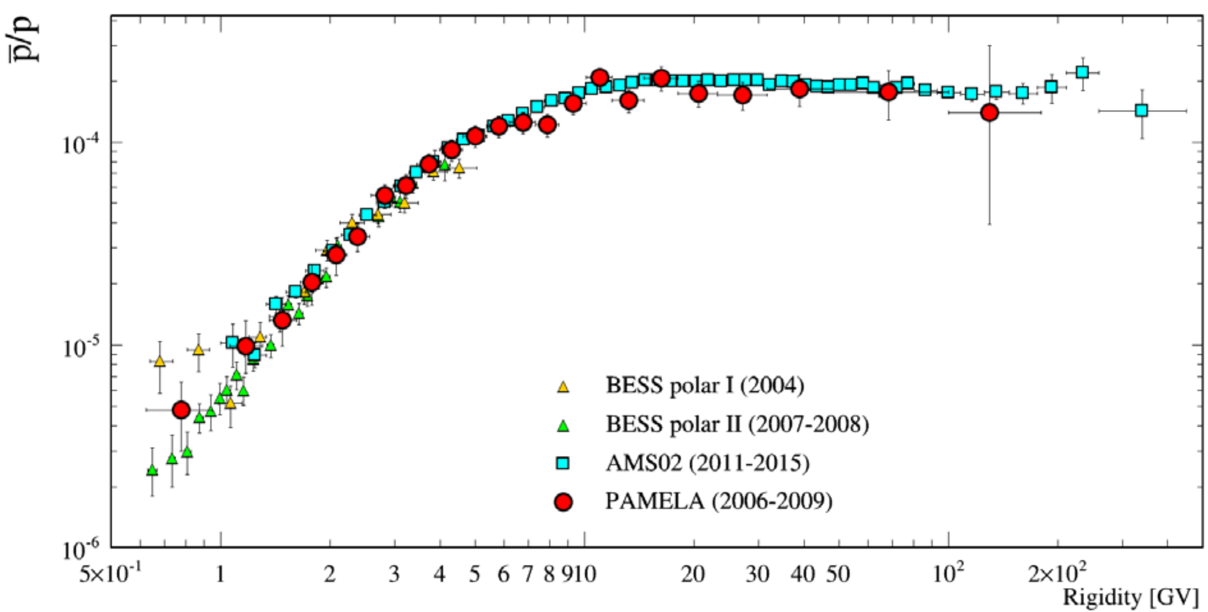

Phenomenological Models for the $\bar{p}/p$ ratio

The precision AMS data allow for exploration of new phenomena

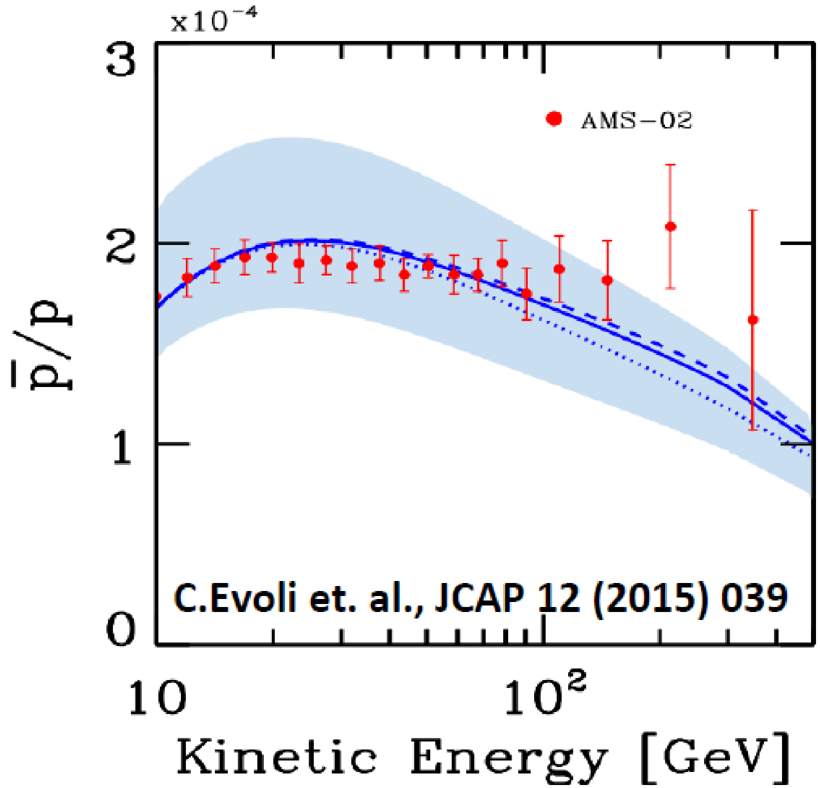

Collision of cosmic rays with interstellar medium:

G.Giesen, et. al., JCAP 09 (2015) 023
C.Evoli et. al., JCAP 12 (2015) 039
R.Kappl, et. al., JACP 10(2015) 034
...

Dark matter contribution to explain the antiproton excess around 10 GV:

A. Cuoco, et. Al.*Phys. Rev. Lett.* 118, 191102
M.Y. Cui, et. al. *Phys. Rev. Lett.* 118, 191101 (2017)

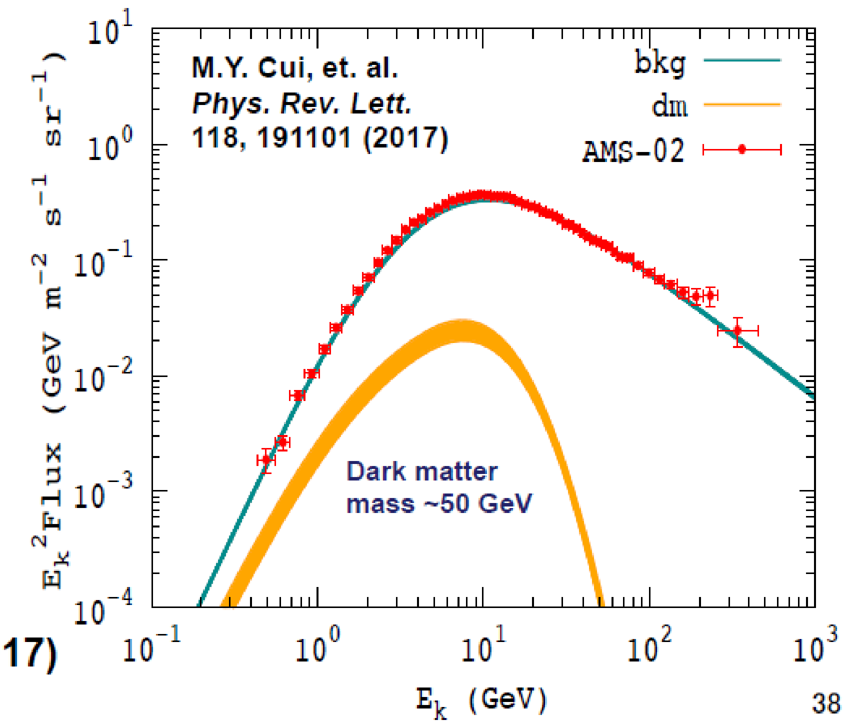

Antiproton Data

G. Giesen et al., JCAP 1509 (2015) 023

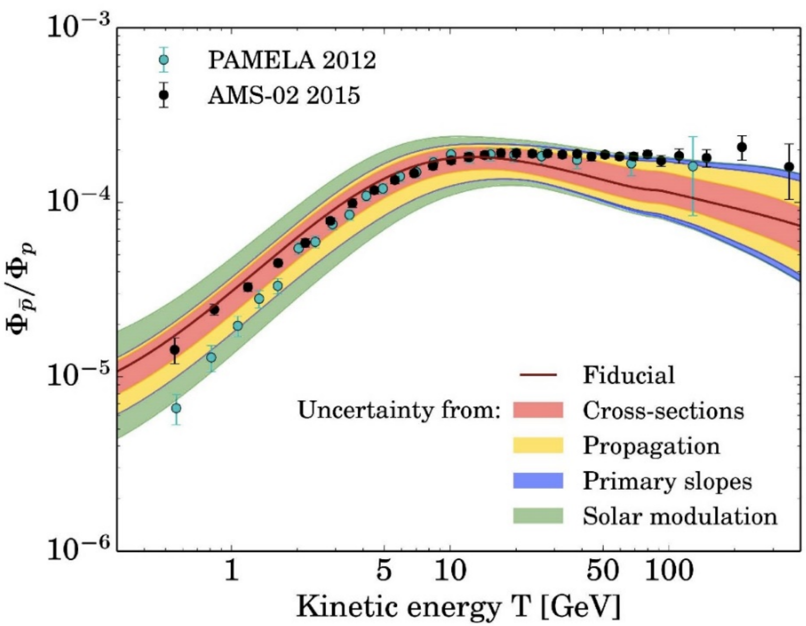

Kappl, Reinert, Winkler JCAP 2015

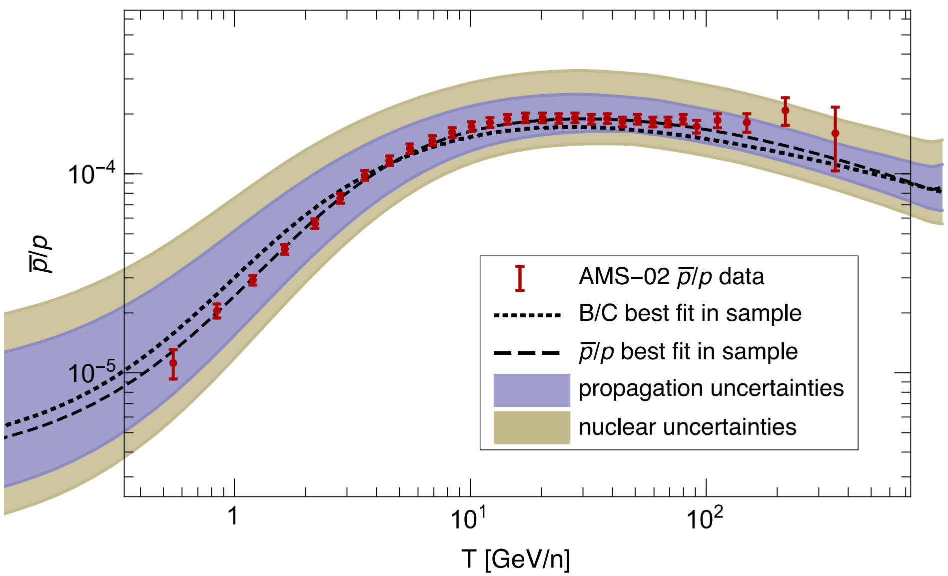

Propagation model fitted on preliminary AMS-02 B/C data
Greatest uncertainty set by nuclear cross sections

Background antiproton can explain data naturally, mainly because of the small diffusion coefficient slope

Diffusion Halo Model

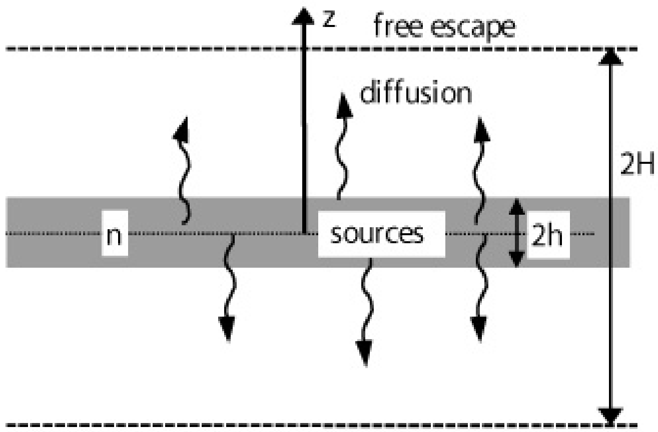

$$\frac{\partial N_i(E,z,t)}{\partial t} = \underbrace{D(E)\cdot\frac{\partial^2}{\partial z^2}N_i(E,z,t)}_{\text{diffusion}} \underbrace{- N_i(E,z,t)\left\{\frac{1}{\tau_i^{\text{int}}(E,z)} + \frac{1}{\gamma(E)\tau_i^{dec}}\right\}}_{\text{interaction and decay}}$$

$$+ \underbrace{\sum_{k>i}\frac{N_k(E,z,t)}{\tau_{\text{int}}^{k\to i}(E,z)}}_{\text{secondary production}} + \underbrace{Q_i(E,z)}_{\text{primary sources}}$$

$$\underbrace{-\frac{\partial}{\partial E}\left\{\left\langle\frac{\partial E}{\partial t}\right\rangle\cdot N_i(E,z,t)\right\} + \frac{1}{2}\frac{\partial^2}{\partial E^2}\left\{\left\langle\frac{\Delta E^2}{\Delta t}\right\rangle\cdot N_i(E,z,t)\right\}}_{\substack{\text{energy changing processes}\\ \text{(ionisation, reacceleration)}}}$$

Fixing the diffusion coefficient: the Boron-to-Carbon ratio

- Li, Be, B are produced by fragmentation of heavier nuclei, mostly C, N, O, on H and He

- B/C is very sensitive to
- propagation effects

B/C = Sec/Prim

$\sim Q_{sec}(E)/Q_{prim}(E)$

$\sim Q_{prim}(E)/D(E) \,/\, Q_{prim}(E)$

$\sim 1/D(E)$

Diffusion coefficient: $D(R)=D_0\beta R^\delta$

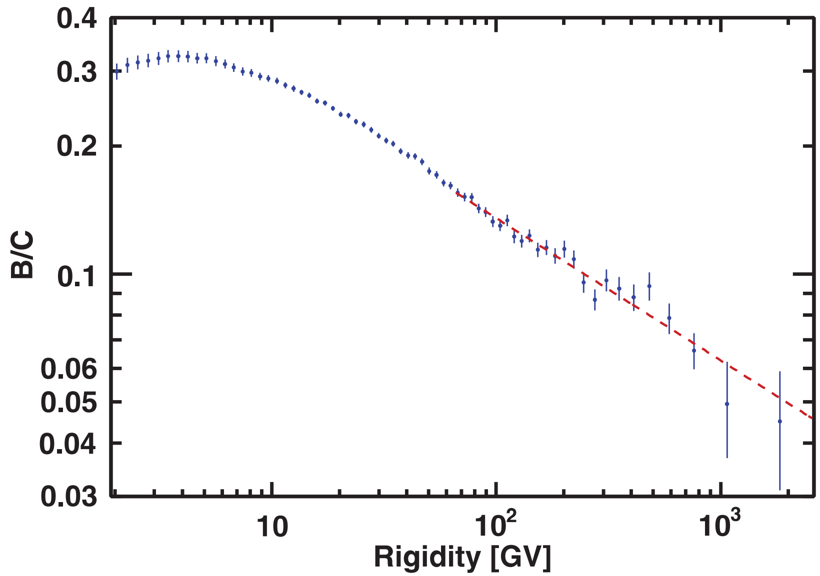

FIG. 1. The AMS boron to carbon ratio (B/C) as a function of rigidity in the interval from 1.9 GV to 2.6 TV based on 2.3 million boron and 8.3 million carbon nuclei. The dashed line shows the single power law fit starting from 65 GV with index $\Delta = -0.333 \pm 0.014(\text{fit}) \pm 0.005(\text{syst})$.

M. Aguilar, PRL 117 (2016) 231102

Courtesy by F. Donato

Transport Equation for the transport, modulation and acceleration of cosmic rays in the heliosphere

$$\underbrace{\frac{\partial f}{\partial t}}\ = \underbrace{\nabla \cdot [\mathbf{K} \cdot \nabla f]}\ - \underbrace{\boldsymbol{V} \cdot \nabla f}\ - \underbrace{\langle \boldsymbol{v}_D \rangle \cdot \nabla f}\ + \underbrace{\frac{1}{3}(\nabla \cdot \boldsymbol{V}) \frac{\partial f}{\partial \ln p}}\ + \underbrace{Q(r,p,t)}$$

Time-dependent, pitch-angle-averaged distribution function

Diffusion

Convection with solar wind

Particle Drifts

Adiabatic energy changes

Any local source

$$\ldots = \ldots + \frac{1}{p^2} \frac{\partial}{\partial p} \left(p^2 D_{pp} \frac{\partial f}{\partial p} \right)$$

Second order Fermi acceleration

Parker (Planet. Space Science, 13, 9,1965)

Courtesy by M. Potgieter

TE in spherical coordinates; diffusion tensor

$$
\begin{aligned}
\frac{\partial f}{\partial t} = & \left[\frac{1}{r^2}\frac{\partial}{\partial r}(r^2 K_{rr}) + \frac{1}{r\sin\theta}\frac{\partial}{\partial\theta}(K_{\theta r}\sin\theta) + \frac{1}{r\sin\theta}\frac{\partial K_{\phi r}}{\partial\phi} - V\right]\frac{\partial f}{\partial r} \\
& + \left[\frac{1}{r^2}\frac{\partial}{\partial r}(rK_{r\theta}) + \frac{1}{r^2\sin\theta}\frac{\partial}{\partial\theta}(K_{\theta\theta}\sin\theta) + \frac{1}{r^2\sin\theta}\frac{\partial K_{\phi\theta}}{\partial\phi}\right]\frac{\partial f}{\partial\theta} \\
& + \left[\frac{1}{r^2\sin\theta}\frac{\partial}{\partial r}(rK_{r\phi}) + \frac{1}{r^2\sin\theta}\frac{\partial K_{\theta\phi}}{\partial\theta} + \frac{1}{r^2\sin^2\theta}\frac{\partial K_{\phi\phi}}{\partial\phi}\right]\frac{\partial f}{\partial\phi} \\
& + K_{rr}\frac{\partial^2 f}{\partial r^2} + \frac{K_{\theta\theta}}{r^2}\frac{\partial^2 f}{\partial\theta^2} + \frac{K_{\phi\phi}}{r^2\sin^2\theta}\frac{\partial^2 f}{\partial\phi^2} + \frac{2K_{r\phi}}{r\sin\theta}\frac{\partial^2 f}{\partial r\partial\phi} \\
& + \frac{1}{3r^2}\frac{\partial}{\partial r}(r^2 V)\frac{\partial f}{\partial \ln p} + Q_{source}(r,\theta,\phi,p,t)\,, \qquad (4)
\end{aligned}
$$

The diffusion tensor can then be written as: (r,θ,ϕ) is:

$$
\begin{bmatrix} K_{rr} & K_{r\theta} & K_{r\phi} \\ K_{\theta r} & K_{\theta\theta} & K_{\theta\phi} \\ K_{\phi r} & K_{\phi\theta} & K_{\phi\phi} \end{bmatrix}
\begin{bmatrix} \kappa_{\|} & 0 & 0 \\ 0 & \kappa_{\perp\theta} & \kappa_A \\ 0 & -\kappa_A & \kappa_{\perp r} \end{bmatrix}
\begin{bmatrix} \cos\psi & 0 & -\sin\psi \\ 0 & 1 & 0 \\ \sin\psi & 0 & \cos\psi \end{bmatrix} =
$$

$$
\begin{bmatrix} \kappa_{\|}\cos^2\psi + \kappa_{\perp r}\sin^2\psi & -\kappa_A\sin\psi & \left(\kappa_{\perp r} - \kappa_{\|}\right)\cos\psi\sin\psi \\ \kappa_A\sin\psi & \kappa_{\perp\theta} & \kappa_A\cos\psi \\ \left(\kappa_{\perp r} - \kappa_{\|}\right)\cos\psi\sin\psi & -\kappa_A\cos\psi & \kappa_{\|}\sin^2\psi + \kappa_{\perp r}\cos^2\psi \end{bmatrix}, \qquad (5)
$$

with ψ the spiral angle of the magnetic field with respect to the radial direction. The components of the gradient and curvature drift velocity are:

$$
\begin{aligned}
\langle \mathrm{v}_d \rangle_r &= -\frac{A}{r\sin\theta}\frac{\partial}{\partial\theta}(\sin\theta K_{\theta r}), \\
\langle \mathrm{v}_d \rangle_\theta &= -\frac{A}{r}\left[\frac{1}{\sin\theta}\frac{\partial}{\partial\phi}(K_{\phi\theta}) + \frac{\partial}{\partial r}(rK_{r\theta})\right], \\
\langle \mathrm{v}_d \rangle_\phi &= -\frac{A}{r}\frac{\partial}{\partial\theta}(K_{\theta\phi}), \qquad (6)
\end{aligned}
$$

Courtesy by M. Potgieter

What about the magnetic field?

Modified and Ideal Parker

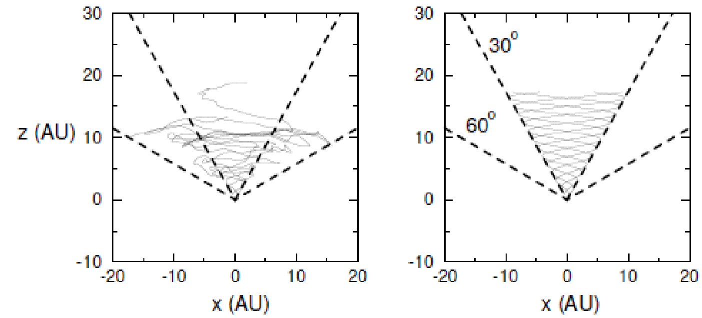

$$
\begin{aligned}
K_{rr} &= \cos^2\zeta\left(\kappa_{\|}\cos^2\psi + \kappa_{\perp,3}\sin^2\psi\right) + \kappa_{\perp,2}\sin^2\zeta, \\
K_{r\theta} &= \sin\zeta\cos\zeta\left(\kappa_{\|}\cos^2\psi + \kappa_{\perp,3}\sin^2\psi - \kappa_{\perp,2}\right) - \kappa_A\sin\psi, \\
K_{r\phi} &= \sin\psi\cos\psi\cos\zeta\left(\kappa_{\perp,3} - \kappa_{\|}\right) - \kappa_A\cos\psi\sin\zeta, \\
K_{\theta r} &= \sin\zeta\cos\zeta\left(\kappa_{\|}\cos^2\psi + \kappa_{\perp,3}\sin^2\psi - \kappa_{\perp,2}\right) + \kappa_A\sin\psi, \\
K_{\theta\theta} &= \sin^2\zeta\left(\kappa_{\|}\cos^2\psi + \kappa_{\perp,3}\sin^2\psi\right) + \kappa_{\perp,2}\cos^2\zeta, \\
K_{\theta\phi} &= \sin\psi\cos\psi\sin\zeta\left(\kappa_{\perp,3} - \kappa_{\|}\right) + \kappa_A\cos\psi\cos\zeta, \\
K_{\phi r} &= \sin\psi\cos\psi\cos\zeta\left(\kappa_{\perp,3} - \kappa_{\|}\right) + \kappa_A\cos\psi\sin\zeta, \\
K_{\phi\theta} &= \sin\psi\cos\psi\sin\zeta\left(\kappa_{\perp,3} - \kappa_{\|}\right) - \kappa_A\cos\psi\cos\zeta, \\
K_{\phi\phi} &= \kappa_{\|}\sin^2\psi + \kappa_{\perp,3}\cos^2\psi.
\end{aligned}
$$

Burger & Hitge 2009

Burger, R. A., T. P. J. Krüger, M. Hitge, and N. E. Engelbrecht, A Fisk-Parker hybrid heliospheric magnetic field with a solar-cycle dependence, *Astrophys. J.*, *674*, 511–519, 2008.

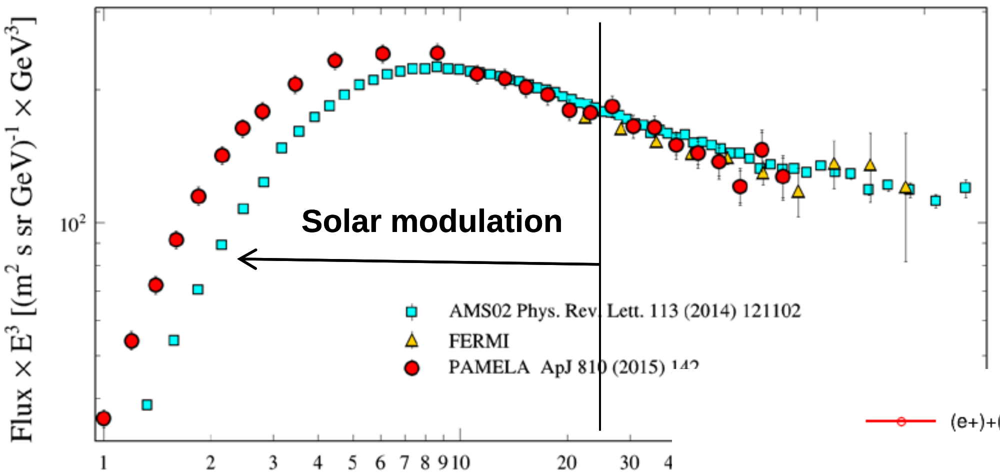

Electron spectrum

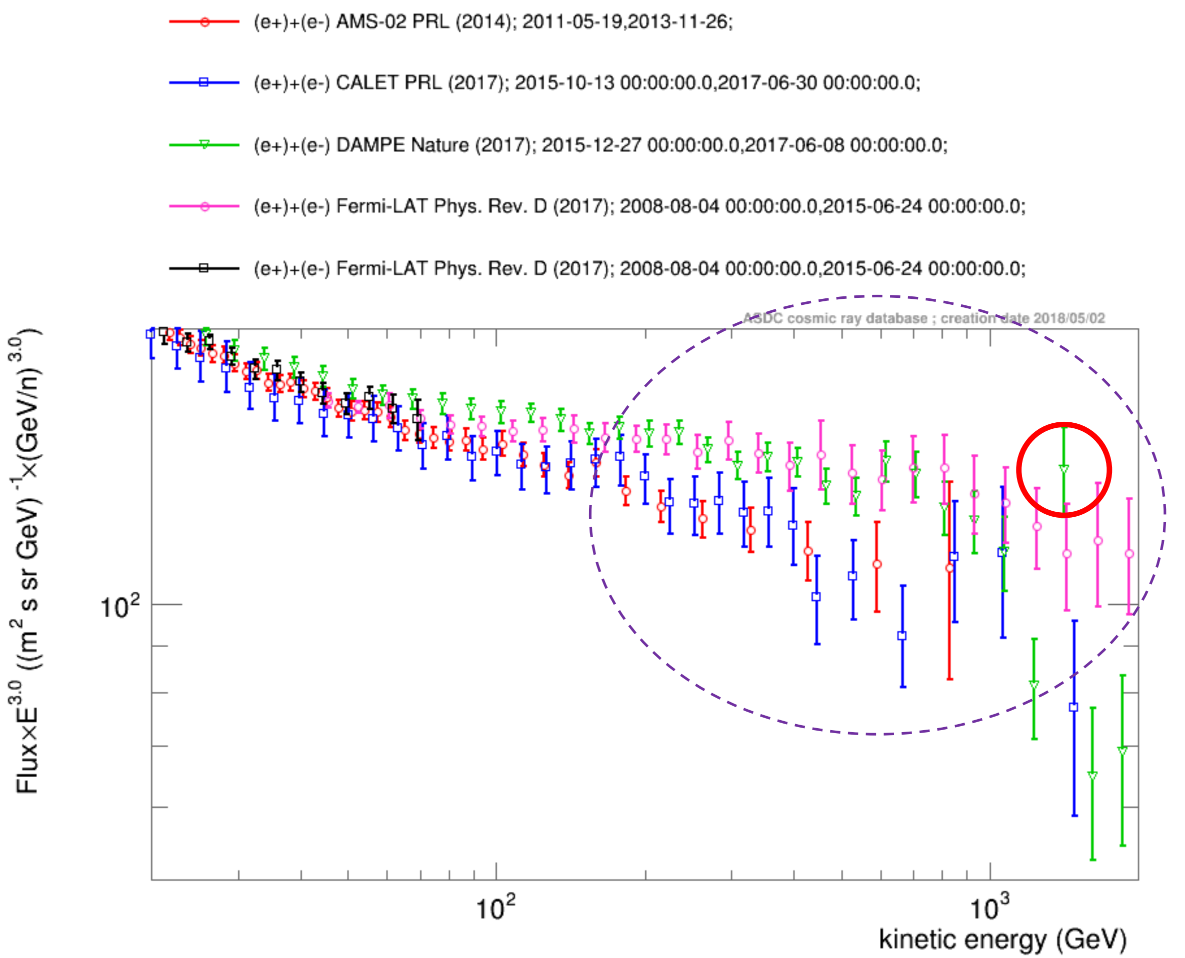

Background “free” Signals?

Why Anti-Deuterium? Background

$$\underbrace{p_{CR}} + \overbrace{p_{ISM}}^{\text{at rest}} \longrightarrow \bar{p}\bar{n} + pn + pp$$

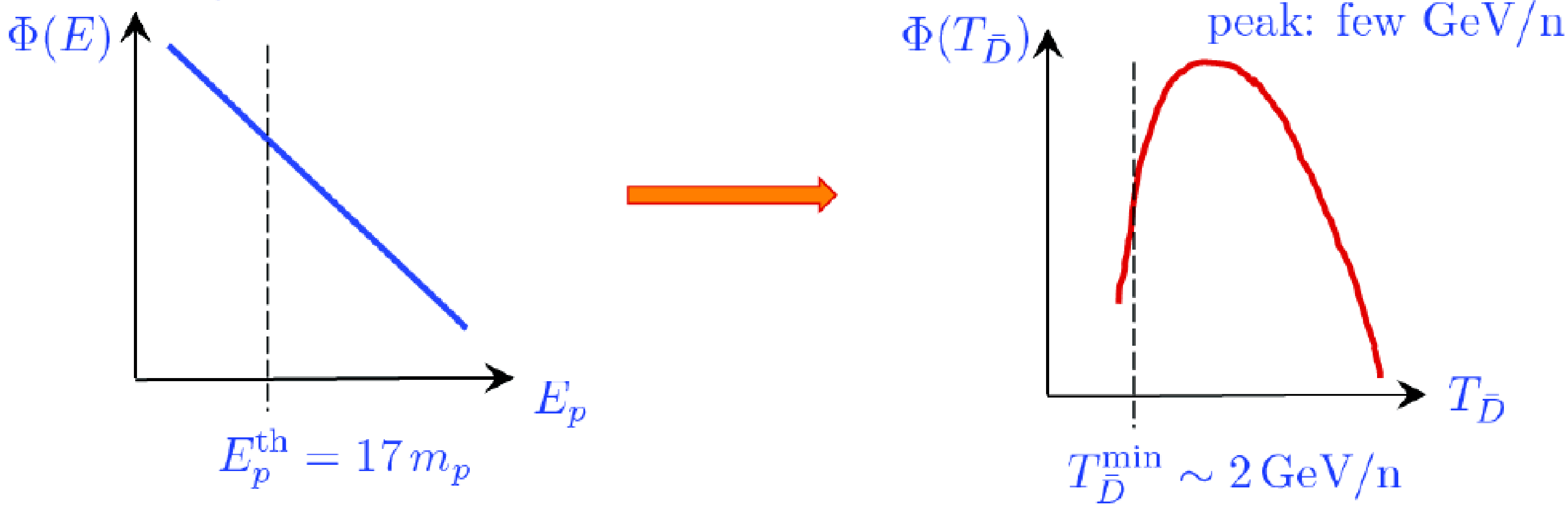

Why Anti-Deuterium? Signal

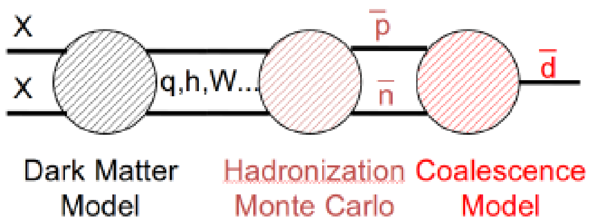

AntiDeuteron Flux

$$\phi(\bar{D}) \propto <\sigma v>_{\text{annihilitaion}} \left(\frac{\rho_{DM}}{M_{DM}}\right)^2$$

$$\otimes (\text{cohalescence } p_0)^3 \otimes \text{propagation}$$

$$\underbrace{\chi}_{\text{at rest}} + \overbrace{\chi}^{\text{at rest}} \longrightarrow \bar{p}\bar{n} + pn$$

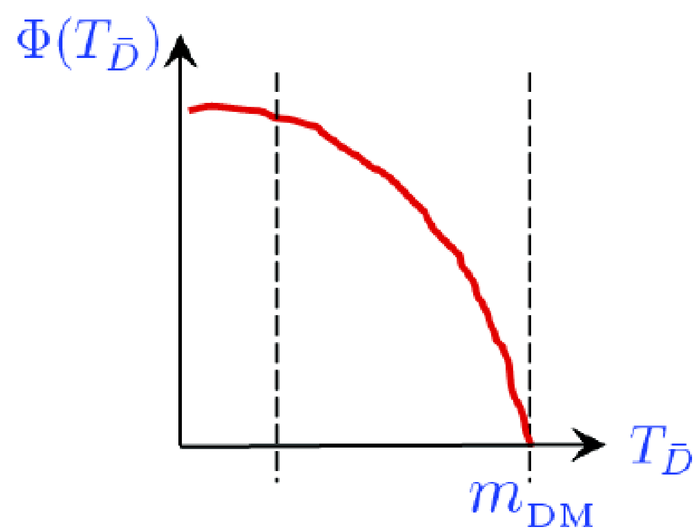

Why Anti-Deuterium? Signal

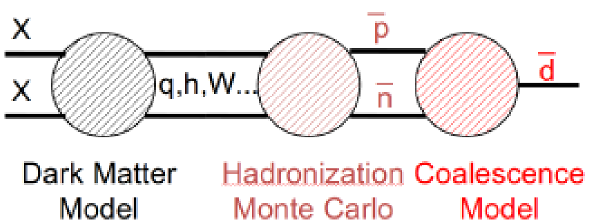

AntiDeuteron Flux

$$\phi(\bar{D}) \propto < \sigma v >_{\text{annihilitaion}} \left(\frac{\rho_{DM}}{M_{DM}}\right)^2 \otimes (\text{cohalescence } p_0)^3 \otimes \text{propagation}$$

$$\underbrace{\chi}_{\text{at rest}} + \overbrace{\chi}^{\text{at rest}} \longrightarrow \bar{p}\bar{n} + pn$$

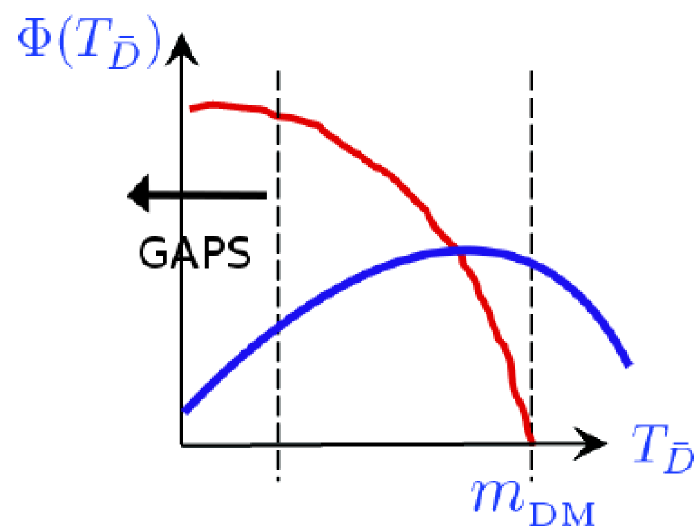

ANTIDEUTERON SENSITIVITY

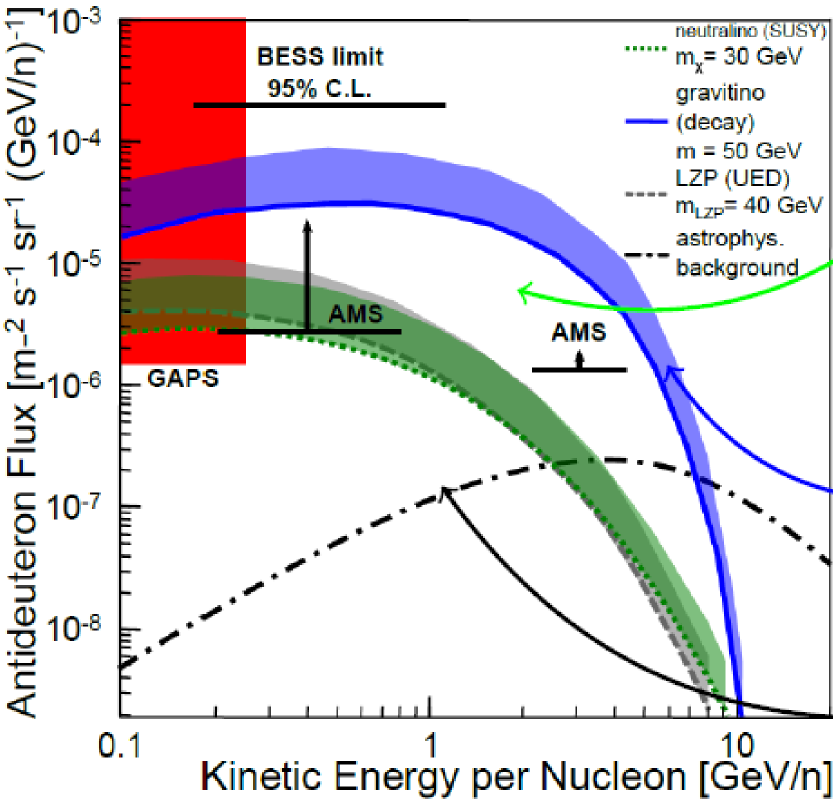

Below .25 GeV/n $\rightarrow$ $\bar{D}$ background $\sim$ 3 orders of magnitude less than the expected signals from DM models.

NEUTRALINO

- SUSY lightest supersymmetric particle, decay into bb, compatible with signal from Galactic Center measured by Fermi

GRAVITINO

- late decays of unstable gravitinos;

ASTROPHYSICAL BACKGROUND

- Collisions of protons and antiprotons with interstellar medium;

Review of the theoretical and experimental status of dark matter identification with cosmic-ray antideuterons arXiv:1505.07785

CR Antihelium

Cirelli, Fornengo, Taoso, Vittino, JCAP2014;   Carlson, Coogan, Linden, Profumo, Ibarra, Wild et al. PRD2014

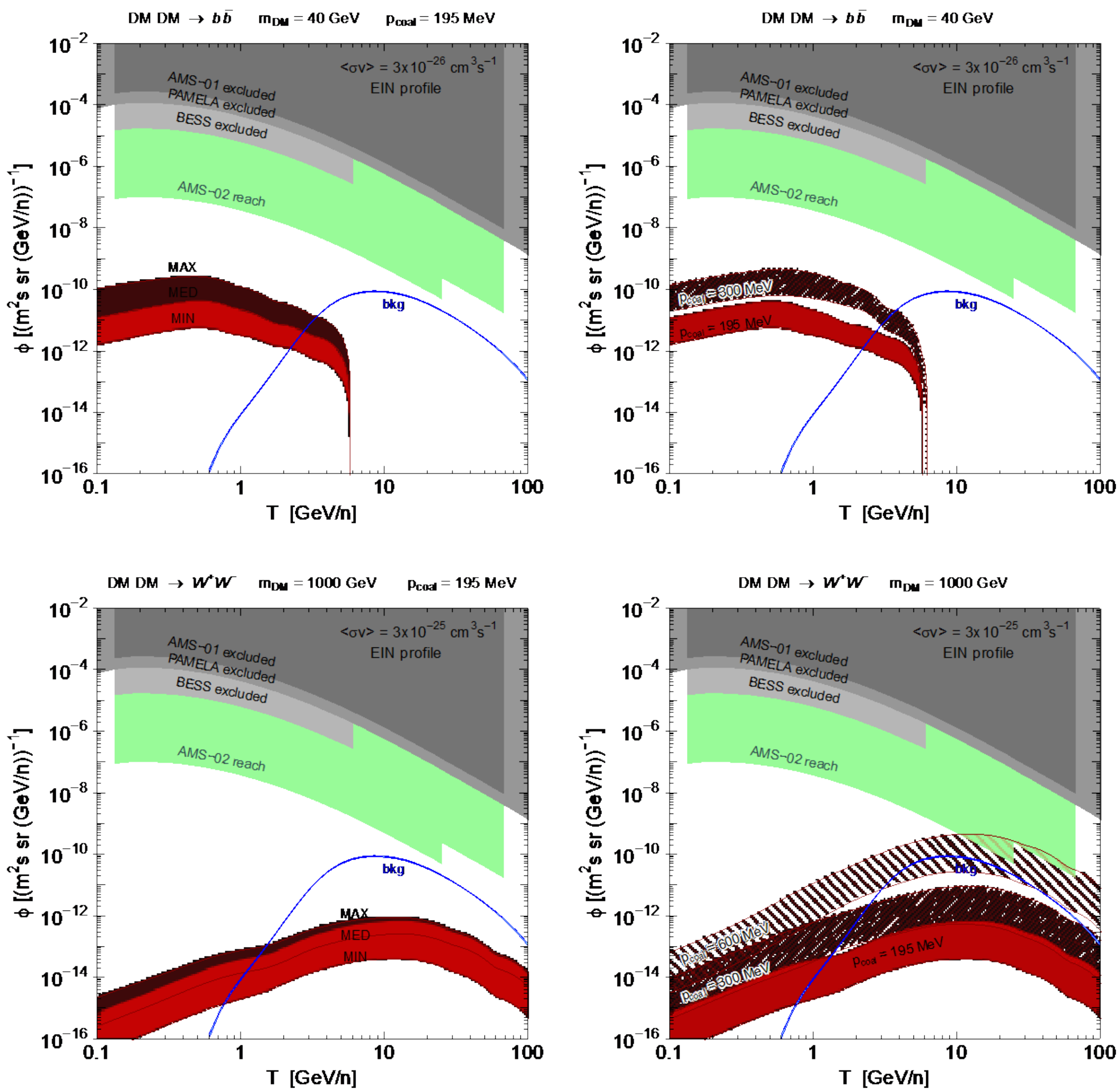

AMS status on complex animatter analysis

To date we have observed a few Z = -2 events with mass around ^{3}He.

The corresponding sample with Z = +2 amount to ~700 million helium events.

At a signal to background ratio of one in one billion, detailed understanding of the instrument is required.

It will take a few more years of detector verification and to collect more data to ascertain the origin of these events.

A. Kounine for the AMS-02 Collaboration, ICRC 2017, Busan, South Korea

PAMELA case: Antiproton / positron identification

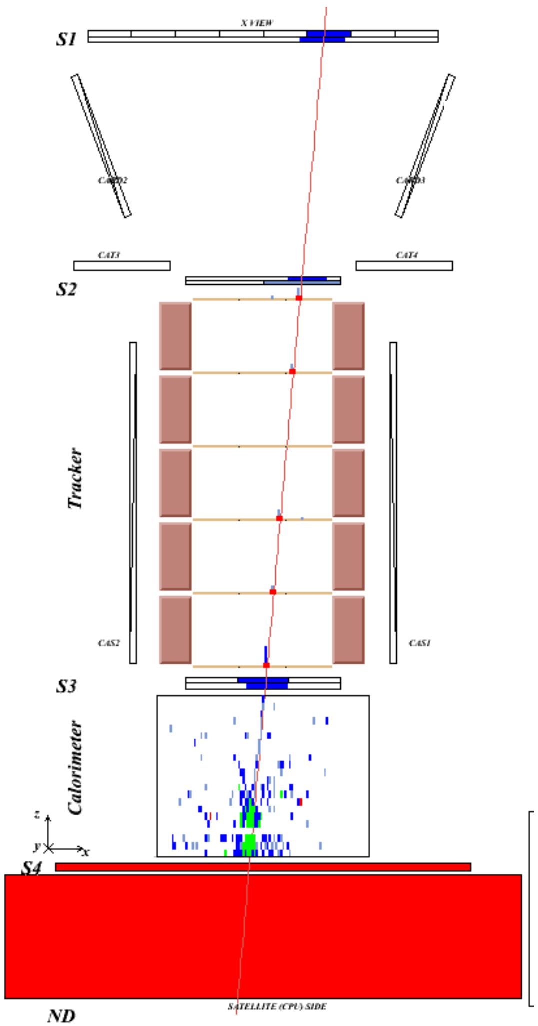

Time-of-flight:
trigger, albedo rejection, mass determination (up to 1 GeV)

Bending in spectrometer:
sign of charge

Ionisation energy loss (dE/dx):
magnitude of charge

Interaction pattern in calorimeter:
electron-like or proton-like, electron energy

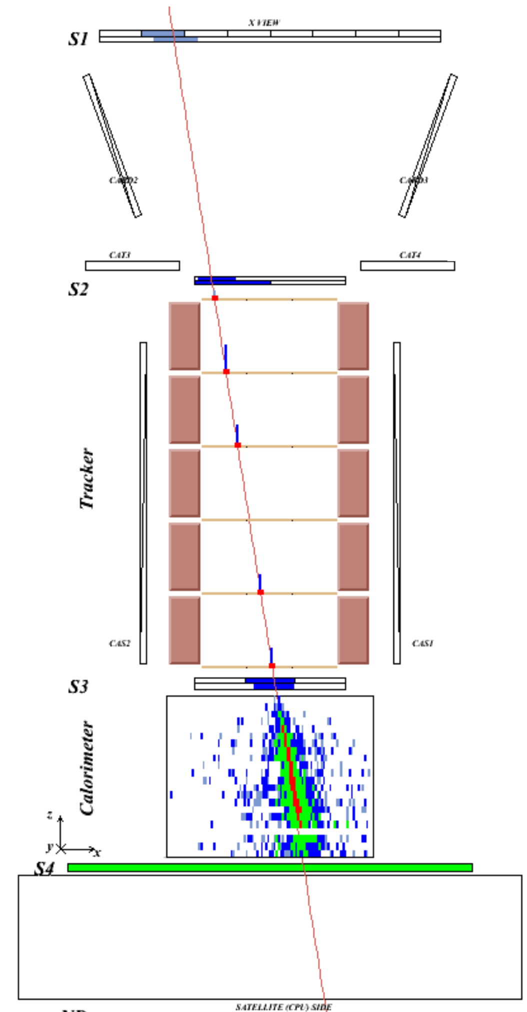

Antiproton
(NB: $e^-/\bar{p} \sim 10^2$)

Positron
(NB: $p/e^+ \sim 10^{3-4}$)

PAMELA Antiproton case: proton 'spillover' background

- Spectrometer tracking information is crucial for high-energy antiproton selection

- Finite spectrometer resolution - high rigidity protons may be assigned wrong sign-of-charge
- Also background from scattered protons

- Eliminate 'spillover' using strict track cuts (χ^2, lever arm, no δ-rays, etc)
- MDR > 10 × reconstructed rigidity

- Spillover limit for antiprotons expected to be ~200 GeV.